REPORT DOCUMENTATION PAGE

Form Approved
OMB No. 0704-0188

1. REPORT DATE *(DD-MM-YYYY)*	**2. REPORT TYPE**	**3. DATES COVERED** *(From - To)*
21/07/2008	Final	03/01/2007-11/30/2007

4. TITLE AND SUBTITLE

ANALYSIS OF FUNCTIONALLY GRADED SHELLS SUBJECTED TO BLAST LOADS

5a. CONTRACT NUMBER
FA9550-07-1-0162

5b. GRANT NUMBER
FA9550-07-1-0162

5c. PROGRAM ELEMENT NUMBER

6. AUTHOR(S)
Romesh C. Batra

5d. PROJECT NUMBER

5e. TASK NUMBER

5f. WORK UNIT NUMBER

7. PERFORMING ORGANIZATION NAME(S) AND ADDRESS(ES)
Virginia Polytechnic Institute and State University

8. PERFORMING ORGANIZATION REPORT NUMBER

9. SPONSORING / MONITORING AGENCY NAME(S) AND ADDRESS(ES)

Air Force Office of Scientific
875 North Randolph Street
Arlington, VA 22203

10. SPONSOR/MONITOR'S ACRONYM(S)

11. SPONSOR/MONITOR'S REPORT NUMBER(S)

12. DISTRIBUTION / AVAILABILITY STATEMENT

DISTRIBUTION STATEMENT A: Approved for public release

13. SUPPLEMENTARY NOTES
None

14. ABSTRACT

The response of doubly curved functionally graded panels exposed to blast loads and a uniform through the wall-thickness temperature field is investigated. Two scenarios, symmetric and antisymmetric about the midsurface, continuous distributions of the two constituent phases, ceramic and metal, are considered, in the sense that in one of them the composition varies gradually from ceramic-to-metal-to-ceramic, while in the other, from ceramic-to-metal. The implications of pressure pulses, volume fraction exponent, panel curvature, and the temperature change on the time-history of the transverse deflection are presented, and pertinent conclusions are drawn.

15. SUBJECT TERMS
Doubly curved shells, functionally graded materials, blast loads

16. SECURITY CLASSIFICATION OF: Unclassified			**17. LIMITATION OF ABSTRACT**	**18. NUMBER OF PAGES**	**19a. NAME OF RESPONSIBLE PERSON**
a. REPORT	**b. ABSTRACT**	**c. THIS PAGE**	None	14	**19b. TELEPHONE NUMBER** *(include area code)*
x					

Standard Form 298 (Rev. 8-98)
Prescribed by ANSI Std. Z39.18

ANALYSIS OF FUNCTIONALLY GRADED SHELLS SUBJECTED TO BLAST LOADS

Abstract

The response of doubly curved functionally graded panels exposed to blast loads and a uniform through the wall-thickness temperature field is investigated. Two scenarios, symmetric and antisymmetric about the midsurface, continuous distributions of the two constituent phases, ceramic and metal, are considered, in the sense that in one of them the composition varies gradually from ceramic-to-metal-to-ceramic, while in the other, from ceramic-to-metal. The implications of pressure pulses, volume fraction exponent, panel curvature, and the temperature change on the time-history of the transverse deflection are presented, and pertinent conclusions are drawn.

1 Introduction

During the last few decades there has been a sustained effort in fabricating aerospace and reusable flight vehicles from advanced laminated composites. However, due to their well-known shortcomings of delamination failure, and chemically unstable matrix and lamina adhesives, especially at high temperatures, new structural paradigms, enabling one to overcome these adverse effects, are needed. Advances in functionally graded materials (FGMs) [1], that combine desirable properties of metals and ceramics, and their applications in aerospace structures, see e.g. [2-6] are being viewed as an alternative solution for aerospace structures exposed to severe thermomechanical environments. In this report, the transient response of shallow doubly curved shells made of FGMs to time-dependent loads induced by an explosion, a sonic-boom or a shock wave is studied.

2 Phase distribution and homogenization of material properties

Points of the shell mid-surface are referred to the Gaussian coordinates x_α, and the thickness coordinate, positive in the downward direction is denoted by x_3.

Based on the rule of mixtures, the effective material property at a point is given by

$$P(x_3) = (P_{\text{ceramic}} - P_{\text{metal}})V(x_3, k) + P_{\text{metal}} \tag{1}$$

where $P(x_3)$ denotes a generic property of the material at a point of the shell, P_{ceramic} and P_{metal} are values of the property for the two phases, ceramic and metal, while $V(x_3, k)$ represents the volume fraction of the ceramic.

The following two scenarios of grading of the ceramic and the metal through the wall thickness are considered:

a) In the case of a high temperature field at both the top the bottom faces of the shell, the phases should vary symmetrically through the wall thickness, in the sense of having 100% ceramic at the outer surfaces of the shell, and tending toward 100% metal at its mid-surface, and

b) In the case of a high temperature at the top surface $x_3 = -h/2$ only, the phases should vary non-symmetrically through the wall thickness. In this case, there is 100% ceramic at the bounding surface $x_3 = -h/2$ of the shell, and 100% metal at the surface $x_3 = h/2$. Here h equals the shell thickness.

Whereas in scenario (a) there is no bending-stretching coupling in the constitutive equations, in scenario (b) such a coupling exits.

For scenario (a), the ceramic volume fraction $V(x_3, k)$ is given by

$$V(x_3,k)=\left(\frac{x_3}{h/2}\right)^k \frac{1+\operatorname{sgn} x_3}{2}+\left(\frac{x_3}{-h/2}\right)^k \frac{1-\operatorname{sgn} x_3}{2} \tag{2}$$

where the signum function is given by $sgn\ (0) = 0$, -1 for $x_3 < 0$, and +1 for $x_3 > 0$; and k, termed the volume fraction index, provides the material variation profile through the wall thickness, $(0 \le k \le \infty)$. Thus, at $x_3 = \pm h/2$, $V = 1$, $P(\pm h/2) \Rightarrow P_c$ for every value of k, and for $x_3 = 0$, $V = 0$ and $P\ (0) \Rightarrow P_m$.

For scenario (b), the composition varies from ceramic to metal, and the variation of V through the wall thickness is represented by

$$V(x_3,k)=\left[(h-2x_3)/2h\right]^k \tag{3}$$

Thus, at $x_3 = h/2$, $P(h/2) \Rightarrow P_m$ and for $x_3 = -h/2$, $P(-h/2) \Rightarrow P_c$. At the midsurface, $x_3 = 0$, and for $k = 1$, $P(0) = (P_c + P_m)/2$.

3 Kinematics and Constitutive Equations

We use the first-order shear deformation theory (FSDT). Accordingly the distribution of 3-D displacements $\mathbf{U}$ through the wall thickness is postulated as [3]:

$$\begin{aligned} U_1(x_1,x_2,x_3,t) &= u_0(x_1,x_2,t)+x_3\ \psi_1(x_1,x_2,t), \\ U_2(x_1,x_2,x_3,t) &= v_0(x_1,x_2,t)+x_3\ \psi_2(x_1,x_2,t), \\ U_3(x_1,x_2,t) &= w_0(x_1,x_2,t). \end{aligned} \tag{4a-c}$$

In Eqs. (4a-c) U_i is the displacement component along the x_i direction; u_0, v_0 and w_0 are displacements of a point on shell's mid-surface, ψ_1 and ψ_2 are rotations about axes x_2 and x_1, respectively, and t is the time variable.

Based on Eqs. (4a-c), the strain field is expressed as

$$\{\varepsilon\}=\left\{\varepsilon^0\right\}+x_3\{\kappa\} \tag{5}$$

where

$$
\begin{aligned}
&\left\{\varepsilon\left(x_\alpha,t\right)\right\}=\left\{\varepsilon_{11},\varepsilon_{22},\gamma_{23},\gamma_{13},\gamma_{12}\right\}^T\\
&\left\{\varepsilon^0\left(x_\alpha,t\right)\right\}=\left\{u_{0,1}-w_0/R_1-\hat{\alpha}\Delta T,v_{0,2}-w_0/R_2-\hat{\alpha}\Delta T,\right.\\
&\qquad\left.w_{0,2}+\psi_2,w_{0,1}+\psi_1,v_{0,1}+u_{0,2}\right\}^T\\
&\left\{\kappa\left(x_\alpha,t\right)\right\}=\left\{\psi_{1,1},\psi_{2,2},0,0,\psi_{1,2}+\psi_{2,1}\right\}^T
\end{aligned}
\qquad \text{(6a-c)}
$$

$\gamma_{ij}(i\neq j)$ denote engineering shear strains, a comma followed by index *j* denotes partial derivative with respect to x_j, $\hat{\alpha}$ is the coefficient of thermal expansion, R_1 and R_2 denote the radii of curvature, and ΔT equals the uniform temperature change from that in the unstressed reference configuration.

Using equations relating the 2-D stress-resultants $\{N\}$ and stress-moments $\{M\}$ to stresses, and assuming that for a shallow shell, $h/R_i \ll 1$, one gets the following expressions:

$$
\begin{aligned}
&\left\{N\right\}=\left[A\right]\left\{\varepsilon^0\right\}+\left[B\right]\left\{\kappa\right\}-\left\{N^T\right\},\\
&\left\{N_{\alpha 3}\right\}=k_s\left[A_s\right]\left\{\gamma_{\alpha 3}\right\},\\
&\left\{M\right\}=\left[B\right]\left\{\varepsilon^0\right\}+\left[D\right]\left\{\kappa\right\}-\left\{M^T\right\},\\
&\left\{N\right\}^T=\left\{N_{11},N_{22},N_{12}\right\},\left\{N_{\alpha 3}\right\}^T=\left\{N_{23},N_{13}\right\},\\
&\left\{\mathrm{M}\right\}^T=\left\{M_{11},M_{22},M_{12}\right\},
\end{aligned}
\qquad (7)
$$

and k_s is the shear correction factor. The superscript *T* on a quantity denotes its value for the thermal field. Matrices $[A],[A_s],[B]$ and $[D]$ are the stretching, the transverse shear, the bending-stretching coupling, and the bending stiffness matrices, respectively. For an FGM, $E = E(x_3)$, $\nu = \nu(x_3)$ and $\alpha = \alpha(x_3)$, where E, ν and α are, respectively, Young's modulus, Poisson's ratio, and the coefficient of thermal expansion. For an orthotropic material, there are nine elastic constants, and three coefficients of thermal expansion.

These constitutive equations are valid for the general distribution of constituent phases across the wall thickness. For the symmetric distribution of constituent phases, the bending-stretching coupling vanishes, and [B] = 0.

4 Governing Equations

We use Hamilton's principle

$$
\delta J=\delta\int_{t_0}^{t_1}\left(\hat{U}-W-T\right)dt=0 \qquad (8)
$$

where t_0 and t_1 are two arbitrary instants of time, $\hat{U}$, W and T denote the strain energy, the work done by surface tractions, edge loads and body forces, and the kinetic energy, respectively, while δ is the variation operator. Equations (5) through (8) yield a system of tenth order partially differential equations, which can be expressed in a compact form as

$$L_{ij}v_j = p_i \qquad \left(i, j = \overline{1,5}\right)$$

Here $L_{ij} = L_{ji}$ are the 2-D differential operators whose expressions are omitted, $p_i\,(t)$ is the thermomechanical load vector, and $v_j = \{u_0, v_0, w_0, \psi_1, \psi_2\}^T$ is the generalized displacement vector.

4 Thermal Blast Loads

A thermal blast load is assumed to be generated by laser heating, and the corresponding temperature rise T is given by

$$\mathrm{T}(r,z,t) = \frac{\mathrm{T}_0}{\sqrt{\mathrm{t}}} e^{-\left(\frac{r}{d}\right)^2} \int_{-\infty}^{t} \frac{e^{-\left(\frac{\tau}{t}\right)^2} e^{-\frac{z^2}{4\kappa(t-\tau)}}}{(t-\tau)^{1/2}} d\tau, \tag{9}$$

where

$$\mathrm{T}_0 = I_m(1-R)(\pi\ \kappa_c\ \rho\ c)^{-1/2} t^{1/2},$$
$$\kappa = \kappa_c/(\rho c),$$
$$z = x_3 + \frac{h}{2},$$

I_m is the laser intensity, R the distance of the laser from the shell surface near the laser, and κ_c the thermal conductivity, ρ the mass density and c the specific heat of the shell material.

For preliminary results presented here, the temperature rise $\Delta\mathrm{T}$ measured from a reference temperature in the stress-free configuration is considered to be time and space independent.

Consistent with the Navier solution to be adopted in the solution of the initial-boundary-value problem, we represent $\Delta\mathrm{T}$ as

$$\Delta T = \sum_{m,n=1}^{\infty} T_{mn} \sin \lambda_m x_1 \ \sin \mu_n x_2$$

where

$$\lambda_m = \frac{m\pi}{L_1}, \quad \mu_n = \frac{n\pi}{L_2},$$
$$T_{mn} = \frac{4(1-(-1)^m)(1-(-1)^n)}{mn\pi^2}\Delta\mathrm{T}, \qquad (10)$$
$$= \frac{16\Delta T}{mn\pi^2}, \qquad (m,n = 1,3,5....).$$

For the thermal stress-resultants N^T and stress couples M^T associated with the FGM, one can use the same representation as for ΔT, that is

$$N^T = \sum_{n,m=1}^{\infty} N_{mn}^T \sin\lambda_m x_1 \ \sin\mu_n x_2,$$
$$M^T = \sum_{n,m=1}^{\infty} M_{mn}^T \sin\lambda_m x_1 \ \sin\mu_n x_2. \qquad (11)$$

Using definitions of N^T and M^T, and assuming the homogenized material to be isotropic, one gets the following expressions for their amplitudes:

$$\left(N_{mn}^T, M_{mn}^T\right) = T_1 \int_{-h/2}^{h/2} E\left(x_3\right)\alpha\left(x_3\right)\left(1, x_3\right)dx_3, \qquad (12)$$

where $T_1 = \dfrac{16\Delta T}{mn\pi^2(1-\upsilon)}$ (m,n=1,3,5....).

For the distribution of volume fractions of constituents given by scenario (a), Eq. (12) simplifies to

$$N_{mn}^T = T_1\Big[E_{cm}\hat{\alpha}_{cm}\left(I_{12}^s + I_{22}^s\right) + \left(E_m\hat{\alpha}_{cm} + E_{cm}\hat{\alpha}_m\right) \times\left(I_{32}^s + I_{42}^s\right)\Big], \qquad (13a)$$
$$M_{mn}^T = 0,$$

and for scenario (b) to

$$N_{mn}^T = T_1\Big[E_{cm}\hat{\alpha}_{cm}I_{12}^a + \left(E_m\hat{\alpha}_m + E_m\hat{\alpha}_{cm}\right)I_{21}^a + E_{cm}\hat{\alpha}_m h\Big],$$
$$M_{mn}^T = T_1\Big[E_{cm}\hat{\alpha}_{cm}I_{12}^a + \left(E_m\hat{\alpha}_m + E_m\hat{\alpha}_{cm}\right)I_{22}^a\Big], \qquad (13b)$$

where $E_{cm} = E_c - E_m$, $\hat{\alpha}_{cm} = \hat{\alpha}_c - \hat{\alpha}_m$, coefficients I_{ij}^S and I_{ij}^a are geometric quantities associated, respectively, with the symmetrically and the asymmetrically distributed volume fractions of the constituents.

5. Mechanical Blast Loads

A mechanical blast load can be generated by an explosion or by a shock-wave disturbance produced by an aircraft flying at a supersonic speed, or by a supersonic projectile, rocket or missile operating in its vicinity. In the latter case, the blast pulse is referred to as sonic-boom. Its time-history is described as an *N*-shape pulse, featuring both a positive and a negative

phase. Since panels considered here have small dimensions, it is reasonable to assume that the pressure is uniform over the entire panel, and that the panel is impacted at normal incidence.

The sonic-boom overpressure can be expressed as

$$p_3(t) = \begin{cases} P_0(1 - t/t_p) & \text{for } 0 < t < \hat{r}t_p, \\ 0 & \text{for t < 0 and t > } \hat{r}t_p, \end{cases} \tag{14}$$

where P_0 denotes the peak reflected pressure in excess of the ambient one, t_p denotes the positive phase duration of the pulse measured from the time of impact of the structure, and $\hat{r}$ denotes the shock pulse length factor.

For $\hat{r} = 1$, the sonic-boom degenerates into a triangular explosive pulse; for $\hat{r} = 2$, a symmetric sonic-boom pulse is obtained, and $\hat{r} \neq 2$ corresponds to an asymmetric *N*-pulse. When $\hat{r} = 1$ and $t_p \to \infty$ in Eq. (14), the *N*-pulse degenerates into a step pulse. Equation (14) can be written in the following equivalent form

$$p_3(t) = P_0\left(1 - \frac{t}{t_p}\right)\left[H(t) - H(t - \hat{r}t_p)\right], \tag{15}$$

where *H(t)* denotes the Heaviside step function.

As a special case of Eq. (15), the rectangular and the step pressure pulses can be obtained. In the former case

$$p_3(t) = P_0\left\{H(t) - H(t - t_p)\right\}, \tag{16a}$$

while for the latter one

$$p_3(t) = P_0 \text{ for } t > 0. \tag{16b}$$

A more realistic expression of the explosive blast pulse as compared to the triangular one is described by the following Friedländer exponential decay equation:

$$p_3(t) = P_0\left(1 - \frac{t}{t_p}\right)e^{-a't/t_p}, \tag{17}$$

where negative phase of the blast is included. In Eq. (17) a′ denotes a decay parameter which is found from the pressure time history measured in the blast test. The triangular explosive load can be viewed as a limiting case of Eq. (17), that is, for $a'/t_p \to 0$.

The sinusoidal pulse

$$p_3(t) = \begin{cases} P_0 \sin \pi t / t_p, & 0 \le t \le t_p \\ 0 & t > t_p \end{cases} \tag{18}$$

will also be considered in numerical simulations.

For an air-blast traveling tangential to the panel, the pressure-time history is represented as

$$p_3(t) = P_0 e^{-\eta(ct - x_1)} H(ct - x_1), \tag{19}$$

where c is the wave speed in the medium surrounding the structure, and η is an exponent determining the character of the blast decay.

6 Solution techniques

We consider a panel with simply supported edges and term the boundary conditions as SS1. That is, on $x_1 = 0, L_1$: $v_0 = 0$; $w_0 = 0$; $\psi_2 = 0$; $N_{11} = M_{11} = 0$ and on $x_2 = 0, L_2$: $u_0 = 0$; $w_0 = 0$; $\psi_1 = 0$; $N_{22} = M_{22} = 0$. The SS1-type boundary conditions imply that edges can move freely in the tangential direction.

The boundary conditions corresponding to simply supported edges are identically fulfilled by expressing the displacements as

$$\begin{aligned} u_0(x_1, x_2, t) &= \sum_{m,n=0}^{\infty} u_{mn}(t) \cos \lambda_m x_1 \sin \mu_n x_2, \\ v_0(x_1, x_2, t) &= \sum_{m,n=0}^{\infty} v_{mn}(t) \sin \lambda_m x_1 \cos \mu_n x_2, \\ \psi_1(x_1, x_2, t) &= \sum_{m,n=0}^{\infty} \psi_{1mn}(t) \cos \lambda_m x_1 \sin \mu_n x_2, \\ \psi_2(x_1, x_2, t) &= \sum_{m,n=0}^{\infty} \psi_{2mn}(t) \sin \lambda_m x_1 \cos \mu_n x_2, \\ w_0(x_1, x_2, t) &= \sum_{m,n=0}^{\infty} w_{mn}(t) \sin \lambda_m x_1 \sin \mu_n x_2. \end{aligned} \tag{20}$$

Consistent with the Navier-type representations (20), we express the load as

$$p_3(t) = \sum_{m,n=1}^{\infty} Q_{mn}(t) \sin \lambda_m x_1 \sin \mu_n x_2,$$

with

$$Q_{mn} = \frac{16}{mn\pi^2} p_3(t) \qquad (m, n = 1, 3, 5, \ldots), \tag{21}$$

where $p_3(t)$ corresponds to the particular case of blast loading.

A generalized displacement $\tilde{V}$ is represented as the sum of two parts, a quasi-static and a dynamic. Thus

$$\tilde{V}(x_1, x_2, t) = \tilde{V}^S(x_1, x_2) + \tilde{V}^d(x_1, x_2, t). \tag{22}$$

Displacements $\tilde{V}^S$ are determined from the governing equations with zero inertia and zero transverse loads. Displacements $\tilde{V}^d$ are determined from the governing equations by keeping the inertia and the transverse dynamic load terms, and discarding thermal terms in the boundary conditions.

7 Numerical Results

7.1 Verification of the Algorithm

In order to verify the computer code, we study vibrations of a plate comprised of a FG material having ZrO_2 and Al as constituents; their material properties are listed in Table 1. We assign very large values to R_1 and R_2 so that the shell like structure can be approximated as a plate. The presently computed frequencies of free vibrations for two values of L_1/h and three values of the shear correction factor are compared with the analytical results of Vel and Batra [7] in Table 2. It is clear that the presently computed frequencies for different modes of vibration are close to the analytical values. Henceforth, we set the shear correction factor equal to $\pi^2/12$.

Table 1. Material Properties

	Modulus(GPa)	Poisson's Ratio	Density(kg/m^3)
ZrO_2	200	0.3	5700
Al	70	0.3	2702

Table 2. Natural Frequencies of a Thick Functionally Graded Shear Deformable Plate, $\left(\varpi = \omega \frac{L_1^2}{h}\sqrt{\frac{\rho_m}{E_m}}\right)$

Volume fraction index, (k=1)	Shear correction factor (k_s)	L_1/h=4			L_1/h=10
		m,n=(1,1)	m,n=(2,2)	m,n=(5,3)	m,n=(1,1)
Present	2/3	5.3884	15.774	38.624	6.1923
	5/6	5.5512	16.852	42.516	6.2305
	$\pi^2/12$	5.5423	16.789	42.281	6.2285
Vel and Batra l[1]	Combined	5.2389	15.772	40.730	5.9980
	MT_m	5.1984	15.611	40.206	5.9609
	SC	5.2405	15.773	40.717	6.0004
	MT_c	5.2888	15.937	41.158	6.0502

7.2 Results and Discussion

The panel material is a combination of aluminum and ceramic. Values assigned to different material and geometric parameters used in the computation of results are listed in Table 3.

Table 3. Material Properties

	Metal (Aluminum)	Ceramic (Alumina)
E, Modulus (GPa)	70	393
υ, Poisson's Ratio	0.3	0.25
ρ, Density (Kg/m^3)	2707	3970
α, Coeff. of Thermal Exp. (/ $^\circ$C)	23×10^{-6}	8.8×10^{-6}
Cv, Specific Heat (J/Kg-$^\circ$K)	900	268
kT, Thermal Cond. (W/m-K)	204	10.4
κ, Thermal Diffusivity (m^2/s)	8.373×10^{-5}	9.783×10^{-6}

($L_1 = L_2 = 0.2$m, h = 0.004m)

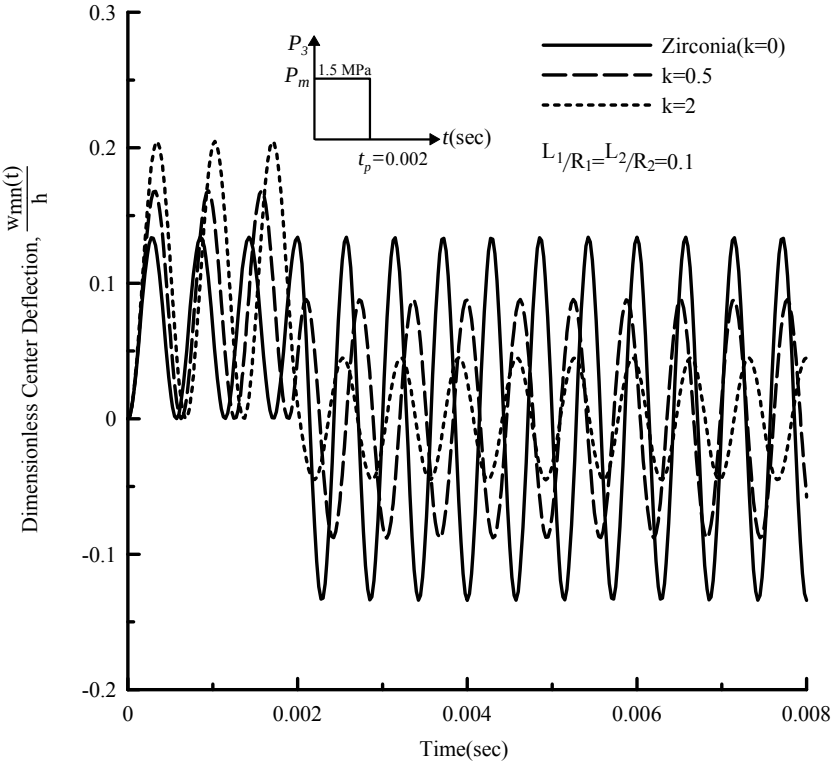

Figure 1: Time histories of the deflection of the shell centroid for three values of the volume fraction index k.

During the computation of results presented below, the temperature is taken to be uniform through the shell thickness and its value is known a priori. Thus the temperature variation only affects the initial deflection of the shell.

7.2.1 Effect of pressure pulse

Figure 1 depicts time histories of the deflection of the shell centroid for three values of the volume fraction index k. The value k = 0 corresponds to a homogeneous material (zirconia). The mechanical shock load is approximated by a rectangular pulse of amplitude 1.5 MPa and time duration 2 ms. During the time the shock pressure acts on the shell, the centroidal deflection for the FG material with k = 2 is the highest of the three cases considered. However, for t > 2 ms when there is no external pressure acting on the shell, the amplitude of the centroidal deflection for the shell made of the homogeneous material is the largest. In each case, the amplitude of vibrations stays constant in time since there is no dissipative mechanism introduced in the problem. We note that the time period of vibrations and hence the frequency depends upon the variation through the thickness of volume fractions of the two constituents.

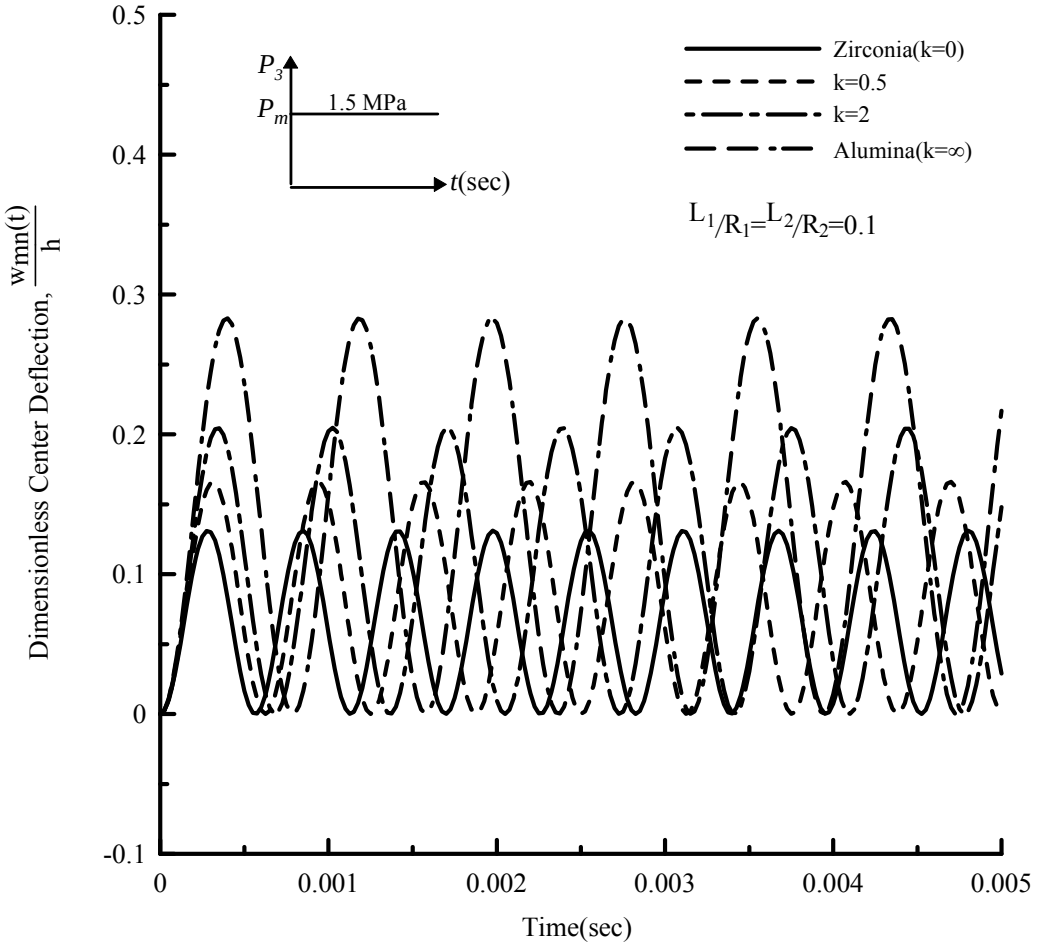

Figure 2: Time histories of the deflection of the shell centroid for four values of the volume fraction index k.

We have plotted in Fig. 2 time histories of the deflection of the shell centroid for a pressure pulse of constant amplitude of 1.5 MPa and for the FG materials for which results are depicted in Fig. 1. The amplitude of the centroidal deflection for the alumina shell is the highest, followed by that of the shell made of the FG material with k = 2. Because the pressure applied to the shell is uniform both in space and time, and there is no dissipative mechanism in the

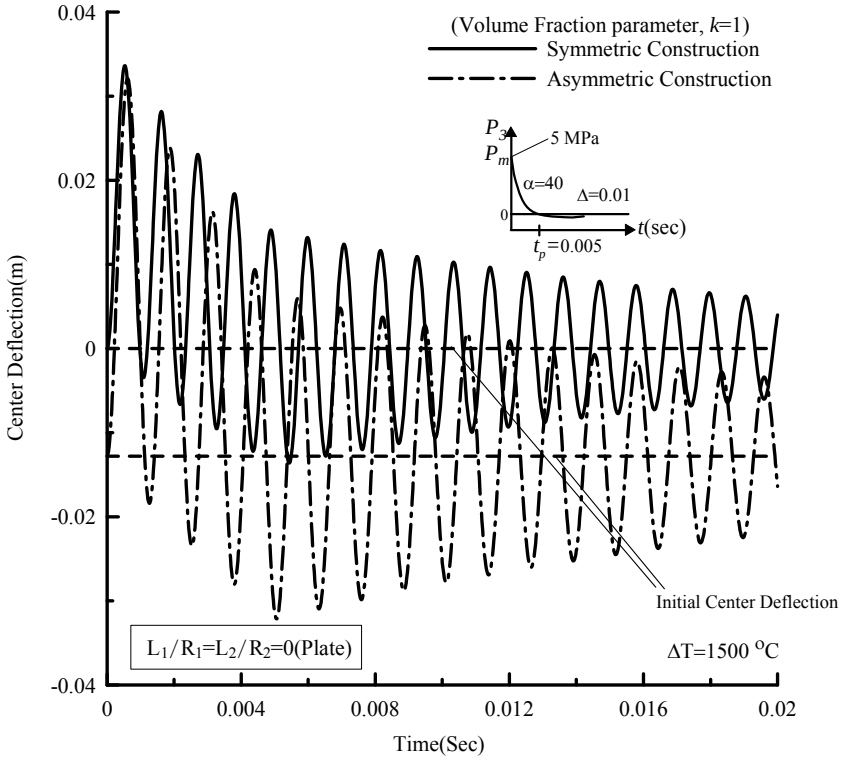

(a)

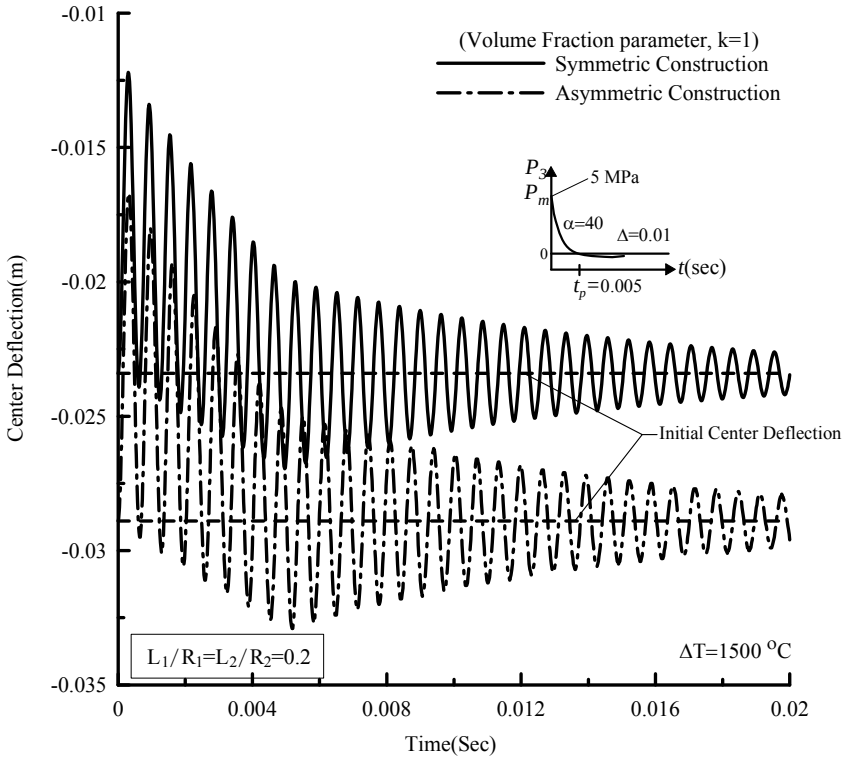

(b)

Figure 3: Time histories of the deflection of (a) the plate, and (b) the shell centroid for symmetric and asymmetric distribution about the midsurface of the two constituents.

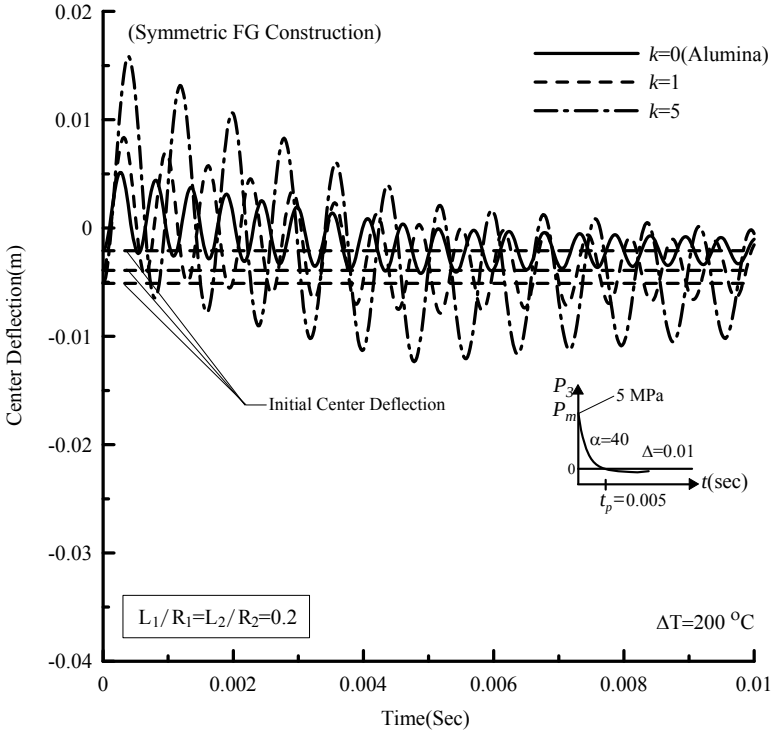

(a)

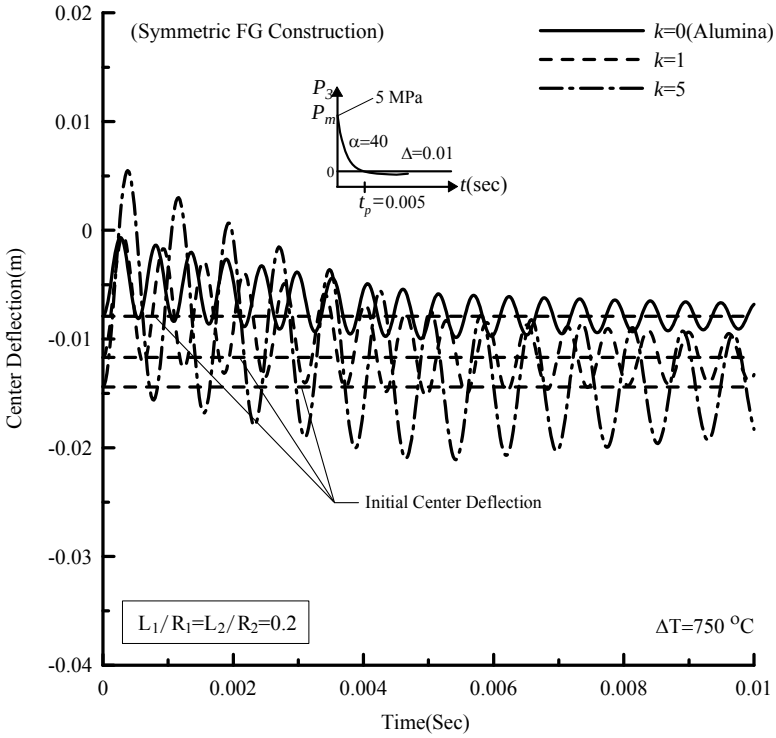

(b)

Figure 4: Time histories of the deflection of the shell centroid for symmetric distribution about the midsurface of the two constituents; (a) $\Delta T = 200\ ^{o}C$, and (b) $\Delta T = 750\ ^{o}C$.

problem, it continues to vibrate about the deformed shape under a statically applied pressure of 1.5 MPa. The maximum deflection of the zirconium shell is 2.2 times that of the aluminum shell even though Young's modulus of zirconium is 5.6 times that of aluminum. Thus inertia forces significantly affect the peak deflection of the shell centroid. We note that the frequency of vibration of a zirconium shell is nearly twice that of the corresponding shell made of aluminum.

7.2.2 Effect of Curvature

For $\Delta T = 1500\ ^{o}C$, and an exponentially decaying pressure pulse of peak amplitude 5 MPa and time duration 5 ms, Figure 3a,b exhibits time histories of the centroidal deflection for a plate and a shell with constituents distributed symmetrically and asymmetrically about the mid-surface of the shell and the same size plate. We note that the asymmetric distribution of constituents results in slightly lower peak deflection as compared to that for the symmetric distribution of the two phases. For the same through-the-thickness distribution of the two phases, the peak initial deflection of the shell with $L_1/R_1 = L_2/R_2 = 0.2$ is about one-third of that of the plate with $L_1/R_1 = L_2/R_2 = 0$.

7.2.3 Effect of Initial Temperature

In Figure 4a,b we have plotted time histories of the centroidal deflection of the FG shell with $L_1/R_1 = L_2/R_2 = 0.2$ and for initial temperatures of $200\ ^{o}C$ and $750\ ^{o}C$ for the symmetric distribution of the material about shell's midsurface; the corresponding results for $\Delta T = 1500\ ^{o}C$ are given in Figure 3b. Except for changing the initial deflection of shell's midsurface, results are both qualitatively and quantitatively the same as is to be expected because of the linear theory employed here.

8. Conclusions

We have studied transient deformations of a doubly curved shell made of a functionally graded material with zirconium oxide and aluminum as the two constituents, and one of the major surfaces of the shell subjected to a mechanical shock load. Three different representations of the blast load are considered; however, the temperature rise is assumed to be uniform throughout the shell and is known a priori. It is found that volume fractions of the two constituents can be suitably tailored to adjust the amplitude of vibrations. Also, for the same distribution of volume fractions of the two constituents, the amplitude of vibrations of the shell is considerably less than that of the corresponding plate.

References

[1] Yamanouchi, M., Koizumi, M., Hirai, T., Shiota, I. (Editors) Proceedings of the First International Symposium on Functionally Gradient Material, Senday, Japan 1990.

[2] Librescu, L. and Song, O., *Composite Thin-Walled Beams: Theory and Application*, Springer, 615 pp., 2005.

[3] Librescu, L., Oh, S-Y. and Song, O., "Thin-Walled Beams Made of Functionally Graded Materials and Operating in a High Temperature Environment: Vibration and Stability," *Journal of Thermal Stresses,* Vol. 28, Nos. 6-7, pp. 649-712, 2005.

[4] Hause, T., and Librescu, L., "Dynamic Response of Anisotropic Sandwich Flat Panels to Explosive Pressure Pulses," *International Journal of Impact Engineering,* Vol. 31, pp. 607-628, 2005.

[5] Hause, T., and Librescu, L., ``Dynamic Response of Doubly-Curved Anisotropic Sandwich Panels Impacted by Blast Loadings," *International Journal of Solids and Structures,* Vol. 44, pp. 6678-6700, 2007.

[6] Librescu, L., Oh, S-Y., and Hohe, J., "Dynamic Response of Anisotropic Sandwich Flat Panels to Underwater and In-Air Explosions," *International Journal of Solids and Structures,* Vol. 43, No. 13, pp. 3794-3816, 2006.

[7] Vel, S.S., Batra, R. C., " Three-dimensional exact solution for the vibration of functionally graded rectangular plates", *Journal of Sound and Vibration*, Vol. 272, pp. 703-730, 2004.